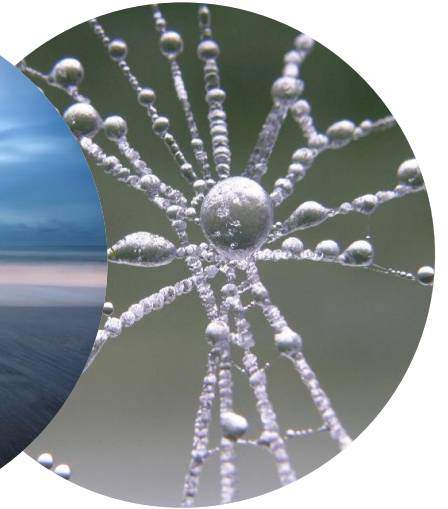
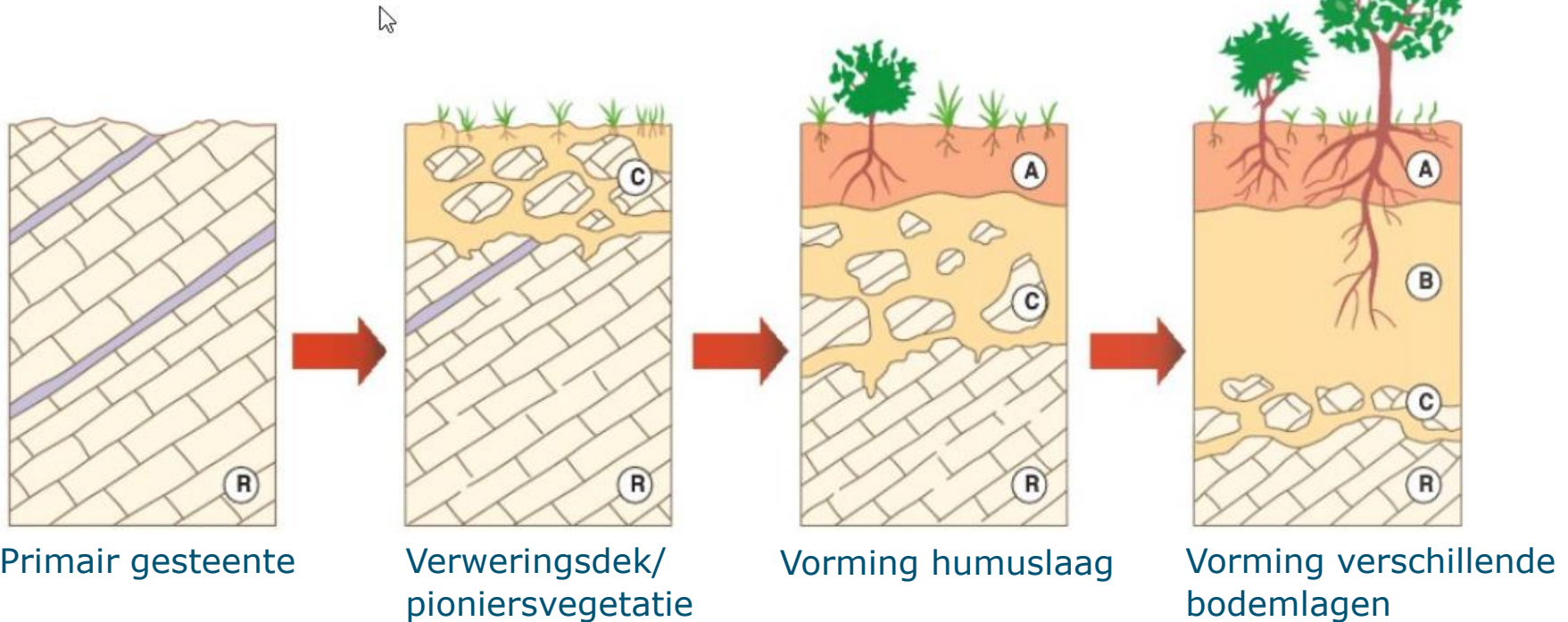


# Structuurvorming monitoren

2 Oktober 2024, Martine van der Ploeg



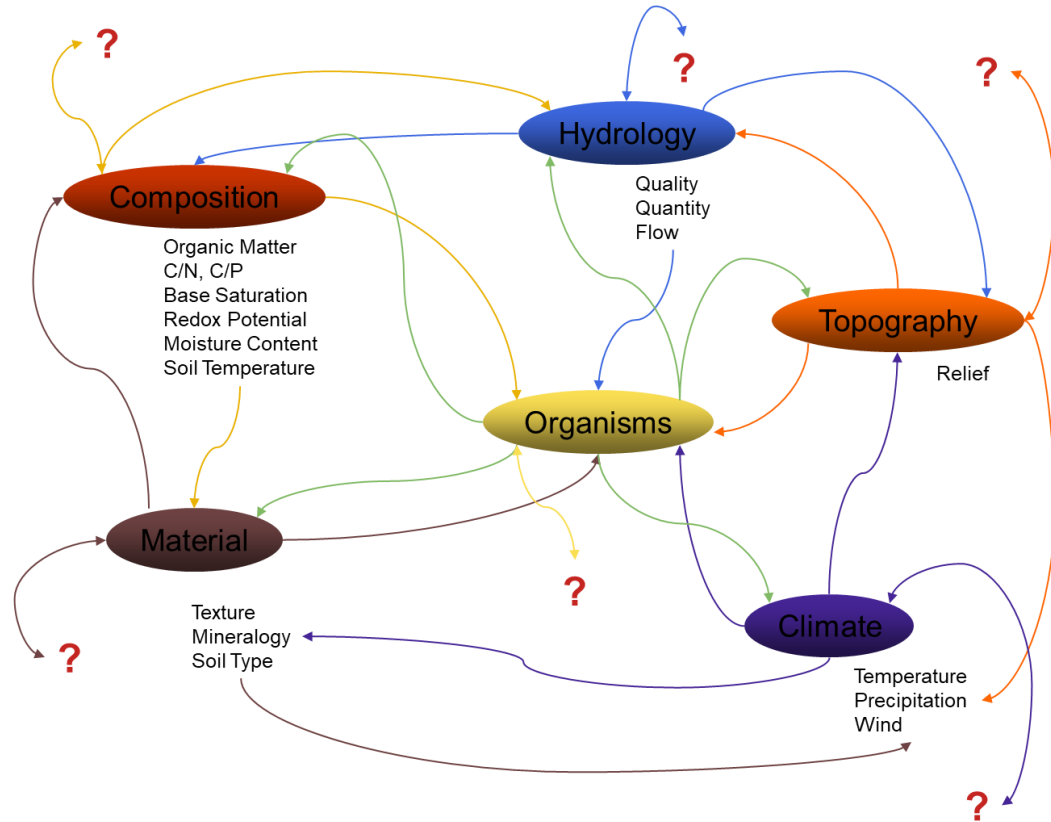
# Bodemvormende processen



# Bodem en structuurvorming bij dijken?



# Natuurlijke bodem en structuurvormende processen



# Extremen structuurvorming: scheuren



Waterkering  
Van Ommerpolder  
in 2018

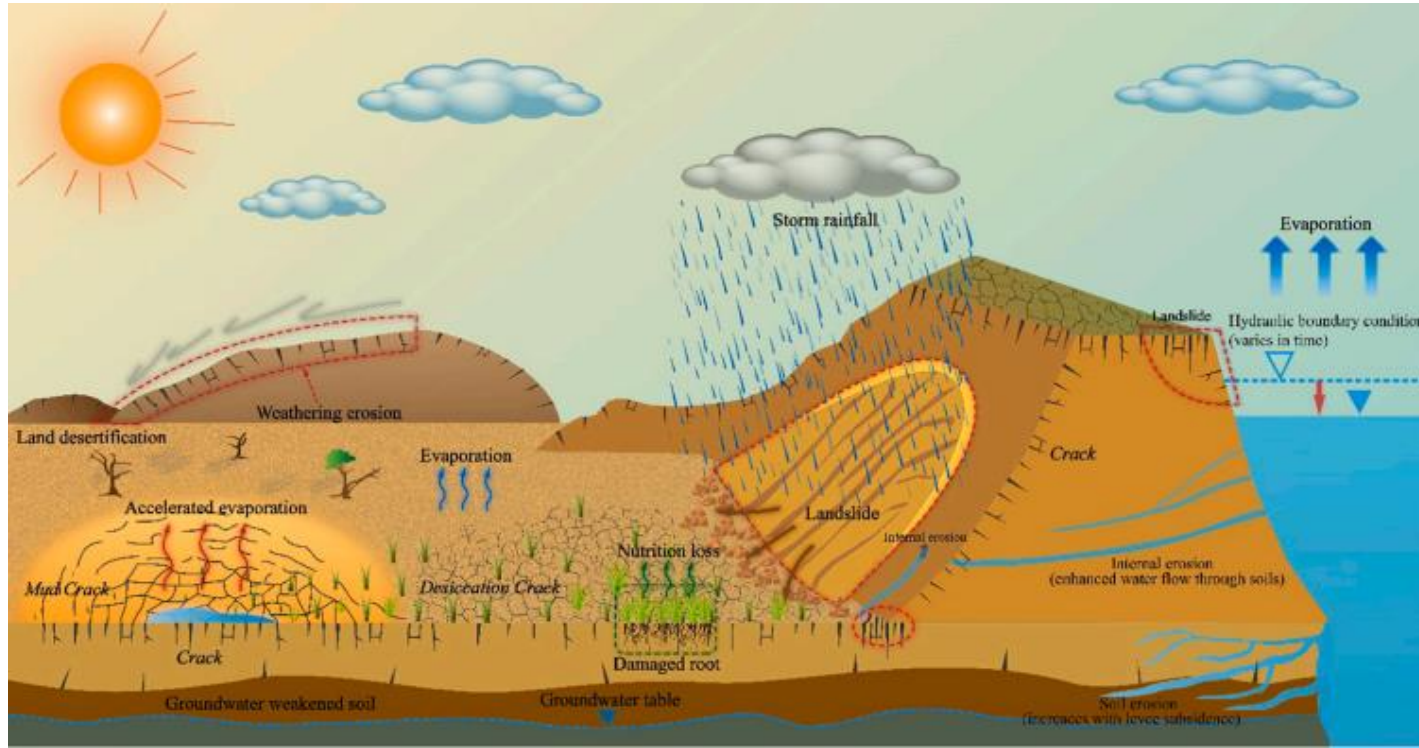
Niek Bosma  
Wetterskip Fryslan

# Extremen structuurvorming: verdichting



Dektares wiki noodmaatregelen

# Mogelijke gevolgen van droogte/verdichting



# Monitoren van structuurvorming

- Aantal voorbeelden vanuit het veld (niet persé dijken), in het lab kan ook van alles maar is vaak anekdotisch en op kleine schaal.
- Voorbeelden dienen ook voor rondvraag naar monitoring structuurvorming
- Discussie later vanmiddag



# Monitoring

- Profielkuilonderzoek



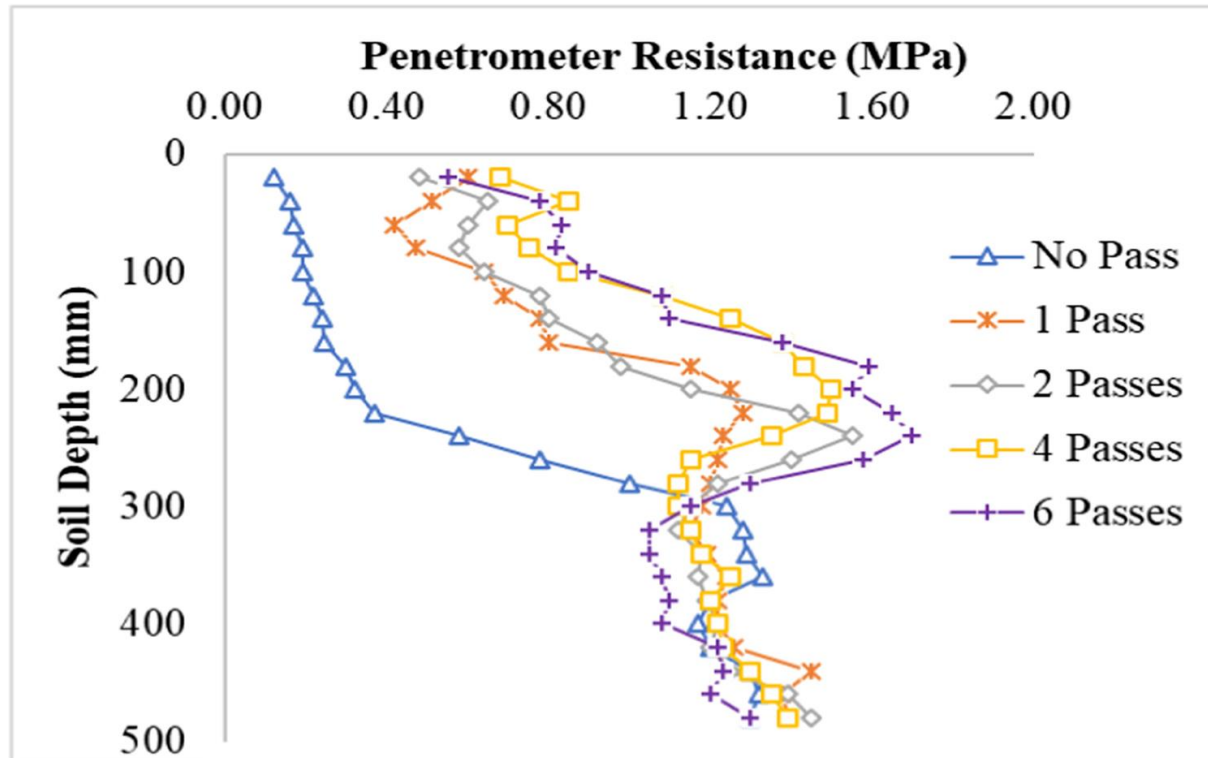
- Penetrometer: Meten van compactie en draagkracht bodem



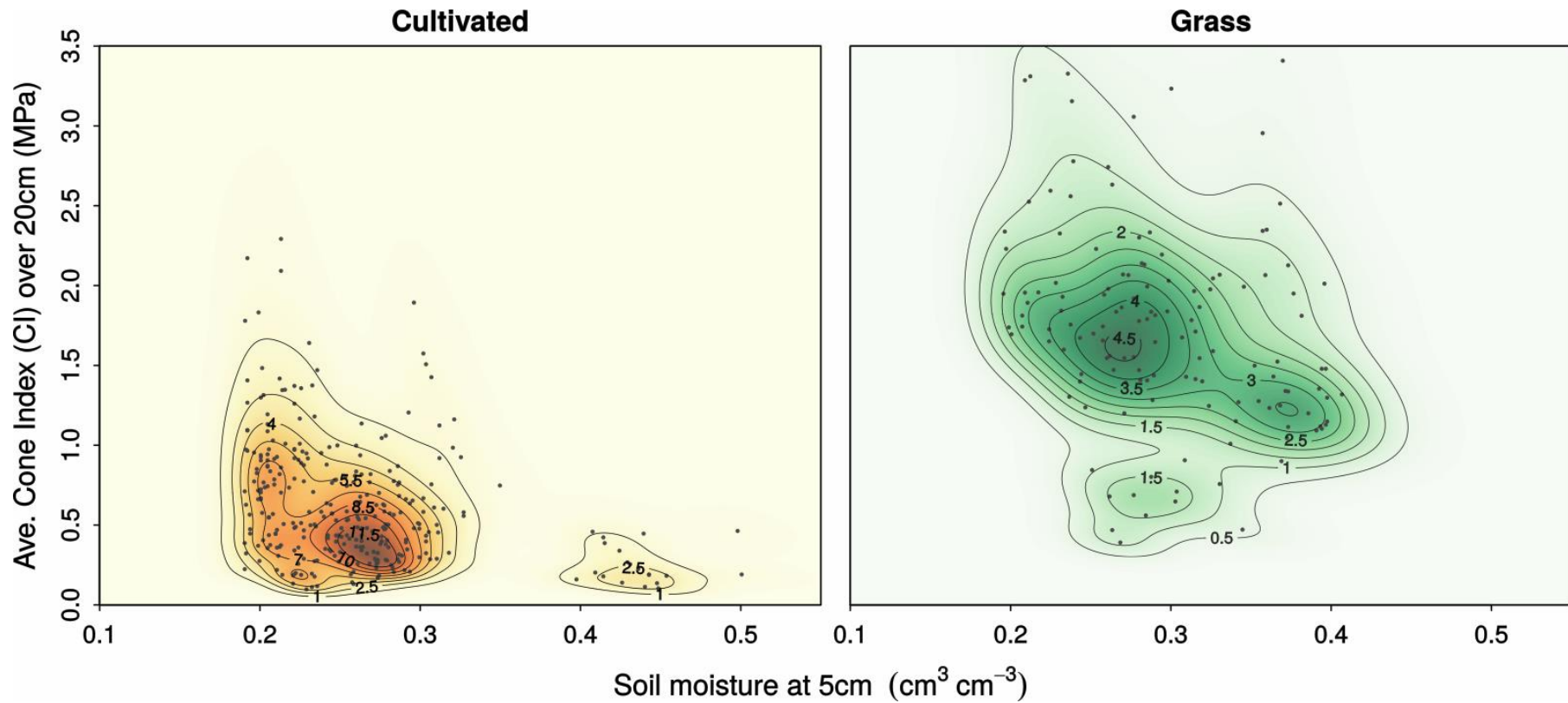
- Compactie door een combine harvester soil van 14.5 Mg/metric ton gemeten met een penetrometer van een geploegd bodem met silt/leem in Wisconsin.

- Shaheb, M.R., Venkatesh, R. & Shearer, S.A. A Review on the Effect of Soil Compaction and its Management for Sustainable Crop Production. *J. Biosyst. Eng.* 46, 417–439 (2021).  
[https://doi.org/10.1007/s42853-021-](https://doi.org/10.1007/s42853-021-00117-7)

00117-7



# Invloed van bodemvocht op penetrometer weerstand



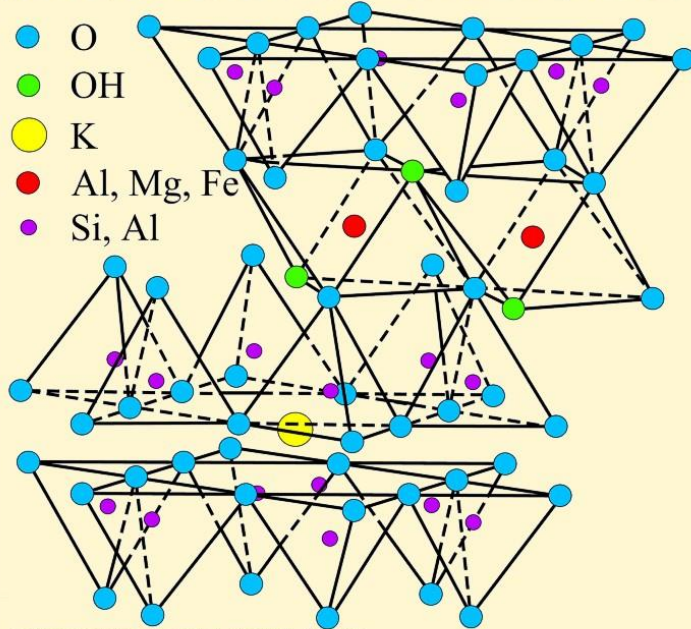
# Kleimineralogie

- Massa % kleimineralen in de lutumfractie (<2  $\mu\text{m}$ ; zonder humus en  $\text{CaCO}_3$ )

|                             | kaolinet | illiet  | vermiculiet | smectiet | chloriet |
|-----------------------------|----------|---------|-------------|----------|----------|
| Rivierklei Rijn             | 5 - 10   | 35 - 40 | 10 - 20     | 10 - 15  | 5 - 10   |
| Zeeklei zoet Zuid Holland   | 5 - 10   | 35 - 40 | 10 - 20     | 10 - 15  | 5 - 10   |
| Zeeklei Friesland/Groningen | 5 - 10   | 30 - 40 | < 5         | 30 - 40  | < 5      |

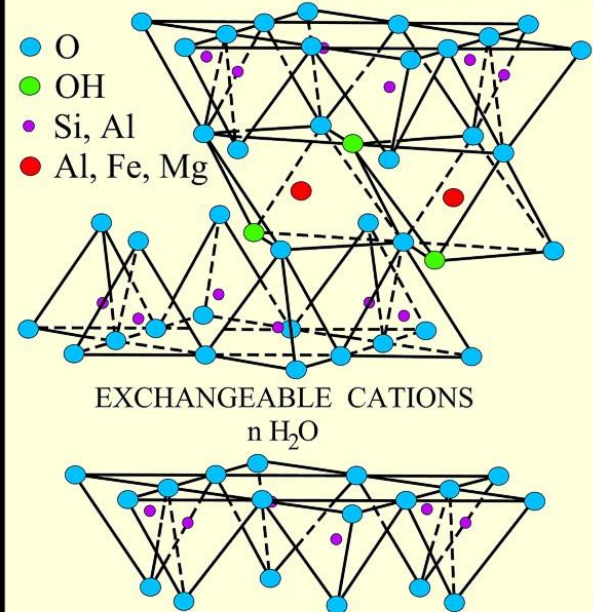
- Vermiculiet en smectiet zijn zwellende/krimpene kleimineralen
  - In Friesland/Groningen is  $\sim 35\%$  van de klei zwellend/krimpene

## STRUCTURE OF ILLITE/MICA



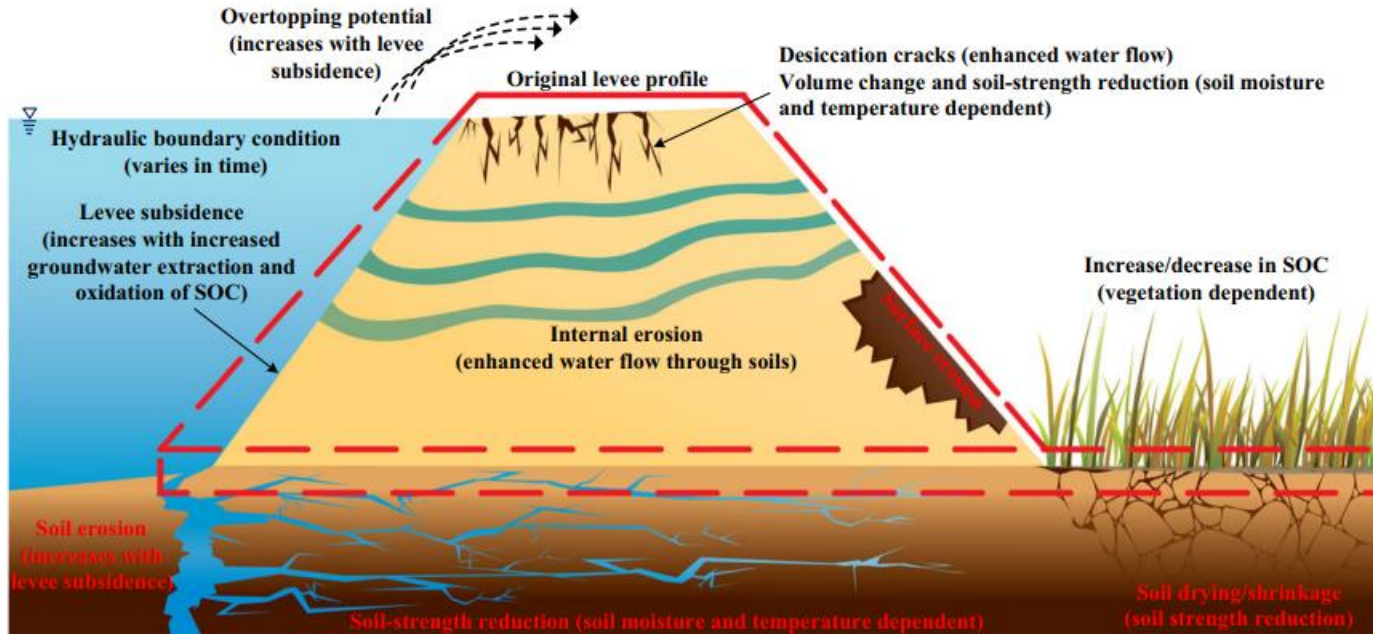
MODIFIED FROM GRIM (1962)

## STRUCTURE OF MONTMORILLONITE

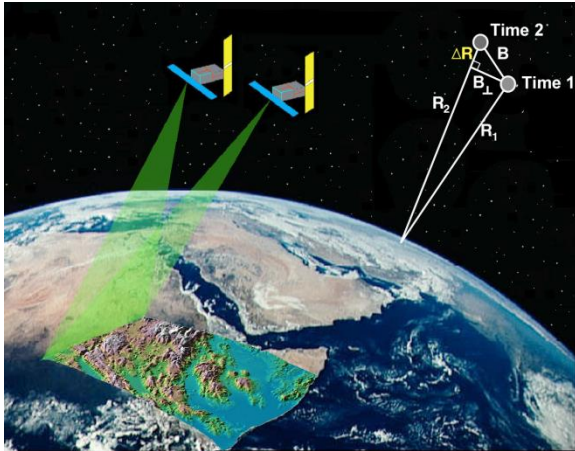


MODIFIED FROM GRIM (1962)

# Gevolgen krimp door droogte



# Monitoren zwel-krimp



1<sup>st</sup> acquisition



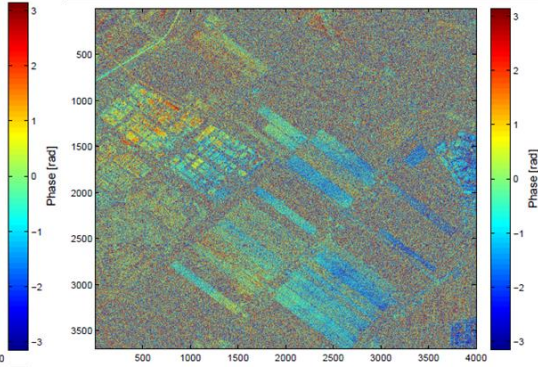
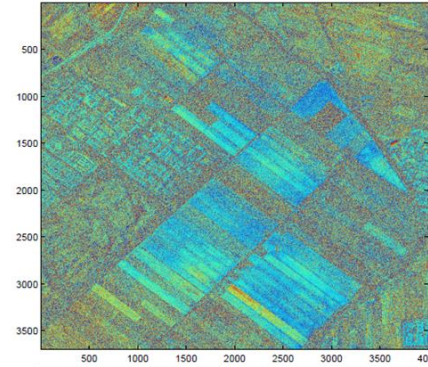
2<sup>nd</sup> acquisition



Phase change: fraction of wavelength  $[-\pi, \pi]$

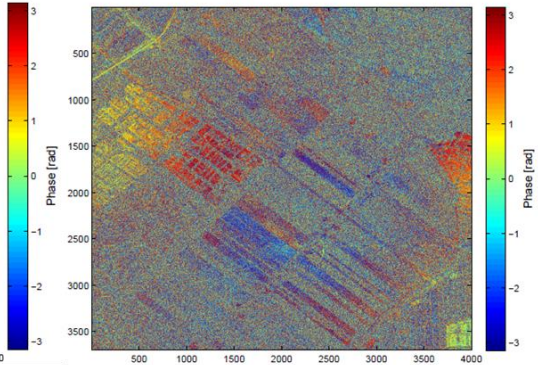
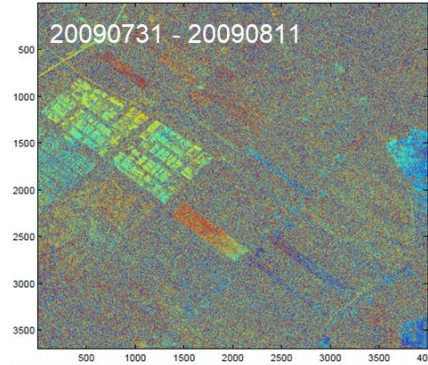


# SRON project: regionale waterbalans

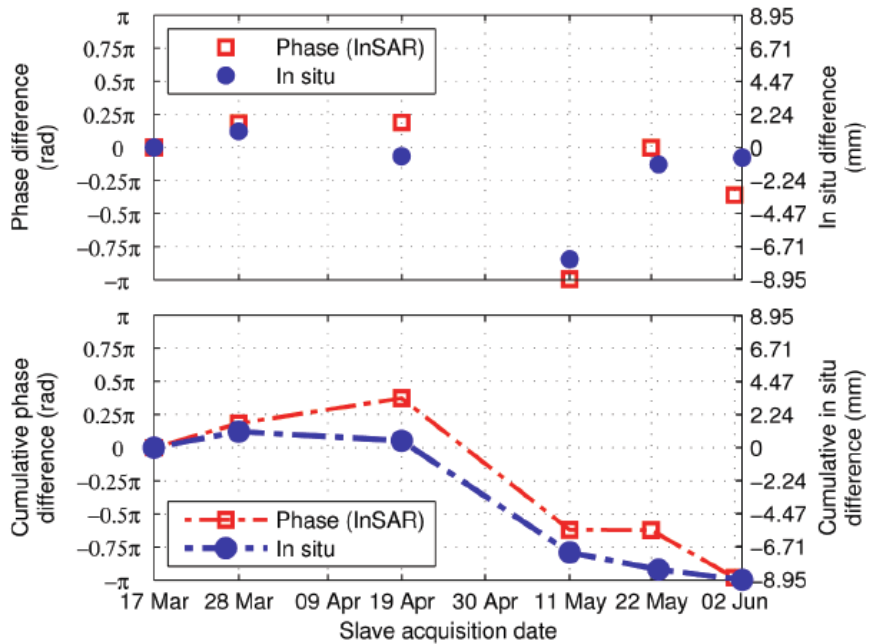


TerraSAR-X data

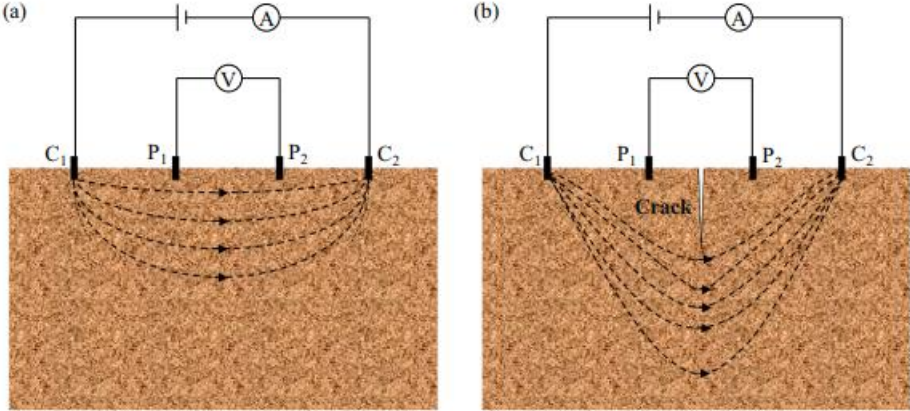
|                    |                      |
|--------------------|----------------------|
| Orbit              | Ascending            |
| Wavelength         | 3.1 cm<br>(9.65 GHz) |
| Spatial resolution | 3 m                  |
| Repeat cycle       | 11 days              |



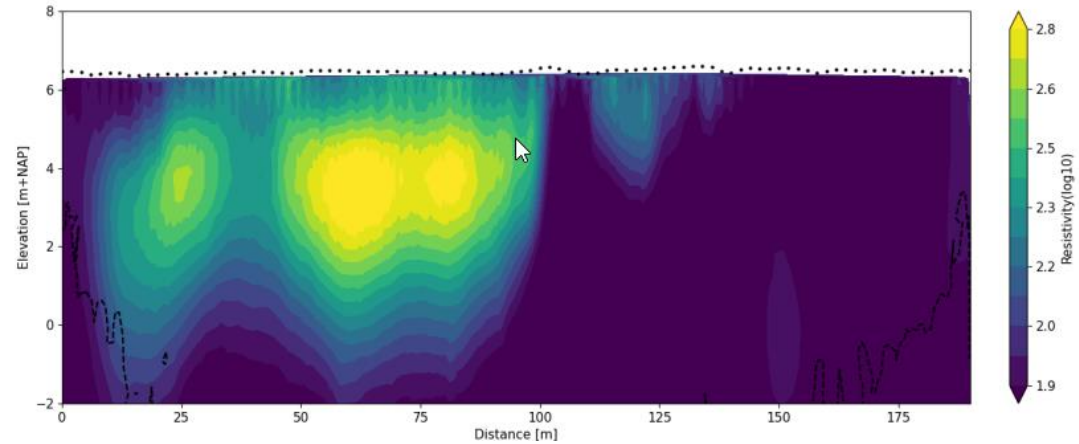
1 colour cycle equivalent to 16 mm line of sight displacement



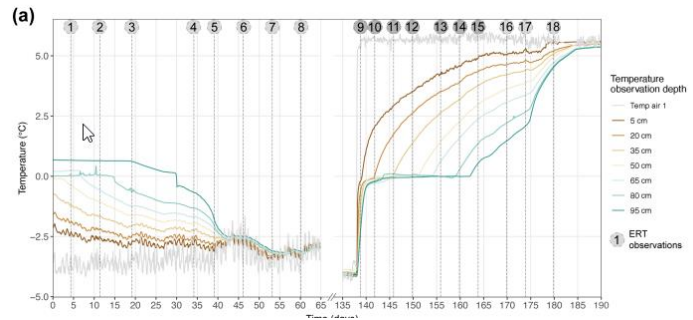
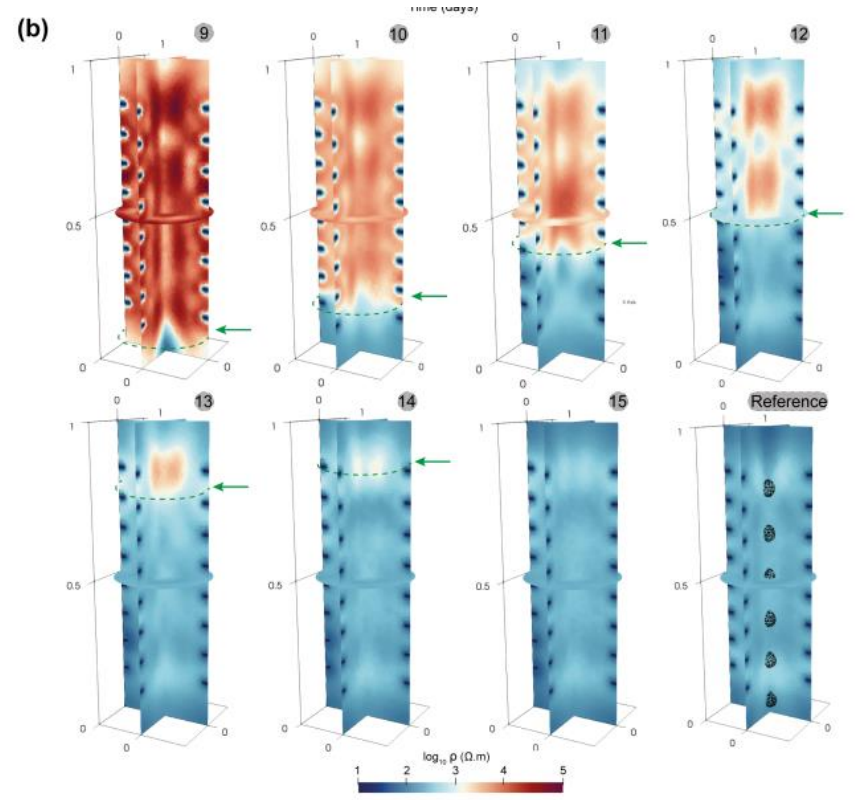
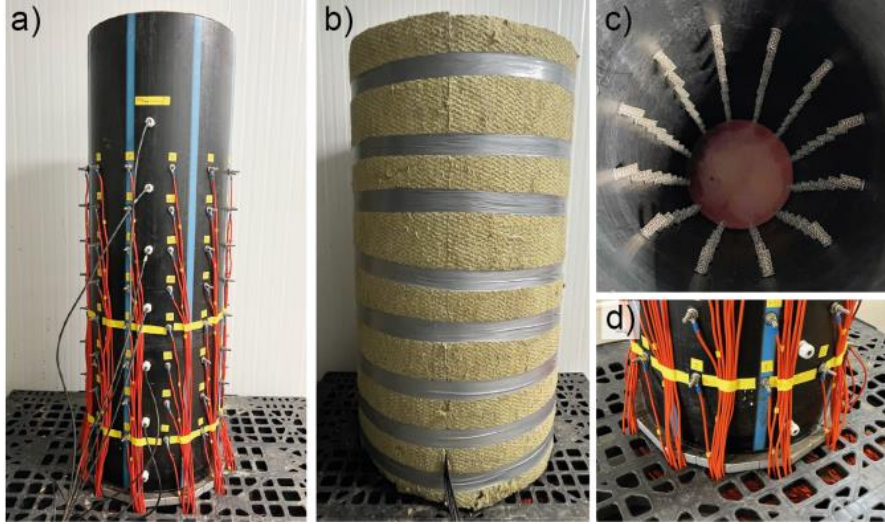
# Electrical resistivity tomography

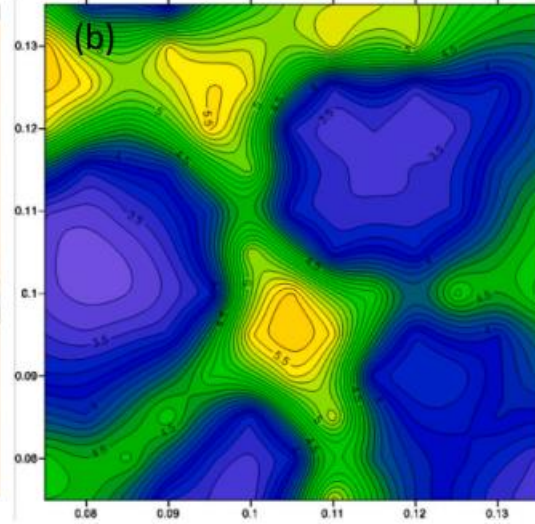
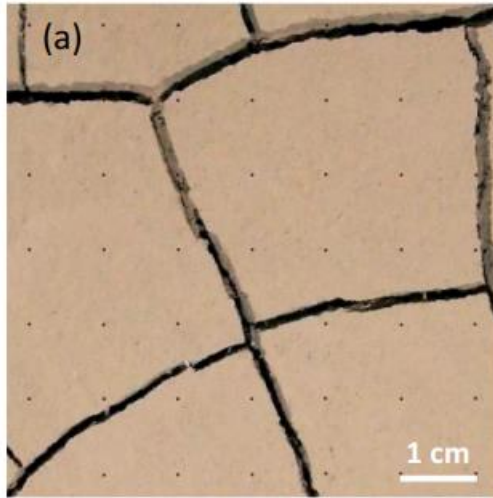


# Grote schaal



# Kleine schaal



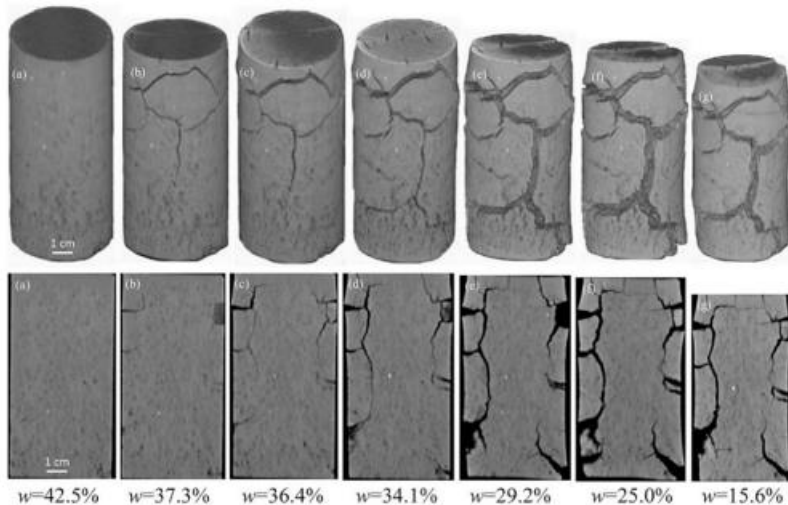


# Uit publicaties

**Table 2**

State of the Art: experimental methods developed to quantify desiccation crack morphology of soils.

| Characterization method                           | Specimen dimension  | Characterization parameter  | References   |
|---|---|---|--|
|   | <ul style="list-style-type: none"> <li>• (L*W*D) (lab/field)</li> <li>• diameter*thickness (lab)</li> <li>• L*W (field)</li> </ul>  |   |  |
| Camera (lab and field)                            | 1.5 m * 1.0 m * 0.5 m (field)<br>400 mm * 7 mm * 5 mm (lab)   | Crack intensity factor<br>Number of cracks, crack width, separation between cracks  | (Miller et al., 1998)<br>(Lecocq and Vandewalle, 2002)   |
|   | 24 cm * 30 cm * 5 mm (lab)<br>160 mm * 160 mm * 5 mm (lab)  | Minkowski numbers, Minkowski functions, angles of bifurcation<br>Number of crack segments and intersections, total/average crack length, average crack width, number of clods, average area of clods, surface crack ratio, probability density functions (PDF), fractal dimension   | (Vogel et al., 2005b)<br>(Tang et al., 2007b)  |
|   | 2.44 m * 2.44 m * 1.22 m (field)<br>1189-297 mm * 841-210 mm * 10-20 mm (field)<br>295 mm * 49 mm * 12 mm (lab)<br>295 mm * 15 mm * 15 mm (lab)   | Crack area, fractal dimension, crack area mass fractal dimension<br>Surface shrinkage, total crack area, average area of cells, total crack length, average crack width, length of crack per unit area<br>Number of cracks, crack-spacing, crack opening, intersecting angle  | (Baer et al., 2009)<br>(Lakshminantha et al., 2009)<br>(Péron et al., 2009b)   |
|   | 16 cm * 16 cm * 8 mm (lab)<br>117 mm * 2.5-5 mm (lab)   | Surface crack ratio, crack intersection angle, number of intersection, number of crack segment, average length of crack, average width of crack, average area of aggregates, crack intensity factor, probability distribution of crack length   | (Tang et al., 2008, 2011a, 2011b; Liu et al., 2013)  |
|   | 100 mm * 5 mm (lab)<br>80 mm * 80 mm * 3-20 mm (lab)<br>180 mm * 210 mm (field)<br>525 mm * 820 mm (field)<br>430 mm * 430 mm * 25 mm (lab)   | Crack intensity factor, density of length of fissure<br>Tensile strain<br>Crack porosity, crack aperture, crack density, density of crack polygon, spatial distribution of crack, crack orientation   | (Trabelsi et al., 2012)<br>(Costa et al., 2013)  |
| Laser device (lab)                                | 9.689 cm * 1.292 cm (lab)<br>7.2 cm * 10.8 cm (lab)<br>9.689 cm * 1.292 cm (lab)<br>80 mm * 40 mm (lab)   | Crack velocity, crack angle, crack width distribution, crack length and density, fractal dimension of the crack network, correlation function of crack area<br>Area of gap, area of crack, area of settlement<br>Crack aperture, crack porosity, specific surface area<br>Surface elevation, crack depth, crack area, soil volume<br>crack specific parameters (depth, length, width, and volume) | (Sánchez et al., 2013)<br>(Ghevenegus et al., 2013)<br>(Sánchez et al., 2013)<br>(Uday and Singh, 2013a)   |
| X-ray Computed Tomography (lab)                   | 40.5 mm * 40.5 mm * 56 mm (lab)<br>12 cm * 12 cm (lab)<br>7.54 cm * 2 cm (lab)<br>50 mm * 100 mm (lab)  | Crack fraction, dead and branch number, crack depth, maximum crack velocity, specific volume<br>crack aperture distributions, crack porosities, and crack specific surface areas<br>Crack area, crack width, crack depth and crack intersection angles<br>Soil mass area, shrinkage ratio, crack ratio, average crack width, total crack length, number of crack segment                          | (DeCarlo and Shokri, 2014a)<br>(Ghevenegus et al., 2011)<br>(Julina and Thyagaraj, 2019)<br>(Tang et al., 2019)                                      |
| Ground penetration radar (field)                  | 1300 mm * 650 mm (field)  | Electrical anisotropy   | (Greve et al., 2010)   |
| Electrical resistivity tomography (lab and field) | 180 mm * 180 mm * 30 mm (lab)<br>29 cm * 3 cm * 2 cm (lab)<br>2.4 dm * 1.7 dm * 1.6 dm (lab)<br>100 m * 6 m (field)<br>49.5 cm * 49.5 cm * 17.5 cm (lab)<br>Petri dish of 10 cm diameter (lab)  | Apparent electrical resistivity<br>Apparent electrical resistivity<br>Apparent electrical resistivity<br>2D and 3D apparent electrical resistivity field<br>3D apparent electrical resistivity<br>Electric field  | (An et al., 2020)<br>(Tang et al., 2018)<br>(Stamouliani et al., 2003)<br>(Jones et al., 2014)<br>(Jones et al., 2012)<br>(Tarafdar and Dutta, 2019) |
| Fiber-optical sensing (lab and field)             | 200 cm * 9 cm * 7 cm (lab)<br>250 mm * 25 mm * 18 mm (lab)<br>117 mm * 117 mm * 8 mm (lab)<br>5.5 cm * 4 cm (lab)   | Surface crack ratio<br>Strain, drying rate<br>Strain field  | (Li and Zhang, 2010)<br>(Costa et al., 2018)<br>(Wang et al., 2018b)   |
| Digital Image Correlation (lab)                   | 100 m * 6 m (field)<br>49.5 cm * 49.5 cm * 17.5 cm (lab)<br>Petri dish of 10 cm diameter (lab)  | Volume strain, local strain<br>Strain field   | (Preh et al., 2010)<br>(Shannon et al., 2015)  |
| Particle image velocimetry (lab)                  | Restrained ring ( $d_{\text{ring}} = 133$ mm; $d_{\text{inner-ring}} = 40$ mm)  | Strain field  |  |
| Scanning Electron Microscopy (lab)                | 20 mm * 20 mm * 20 mm<br>12 cm * 0.5 cm<br>4 mm * 4 mm * 2 mm<br>150 mm * 3 mm<br>600 $\mu\text{m}$ * 600 $\mu\text{m}$ * 2.5/10 mm<br>300 $\mu\text{m}$ * 300 $\mu\text{m}$ * 2.5/10 mm<br>100 $\mu\text{m}$ * 100 $\mu\text{m}$ * 2.5/10 mm | Crack network<br>Local particle alignment<br>Water sensitivity, crack type, clay mineral proportion, dominant clay family<br>Micro crack, salt precipitation pattern<br>crack spacing, crack density, crack length  | (Fauchille et al., 2014)<br>(Mal et al., 2008)<br>(Montes et al., 2004)<br>(Shokri et al., 2015)<br>(Seghir and Ancoet, 2015)                        |
| Field observation                                 | Tens of meters wide and up to 300 m wide polygons<br>Kilometer-scale<br>1-30 m wide   | Large desiccation polygons in playas in California, USA<br>Giant cracks on Mars<br>Image obtained from the imaging spectrometer orbiting Mars   | (Neal et al., 1968)<br>(McGill and Hills, 1992; Pechmann, 1980)<br>(El-Maarry et al., 2015a, 2015b, 2015c)<br>(Stein et al., 2018)                   |
|   |   | Maximum width, vertex angles  |  |



# Monitoren structuurvorming?

